

N62-15055

N62-15055

NASA TN D-1169

NASA TN D-1169



10

TECHNICAL NOTE

D-1169

DESIGN AND CALIBRATION OF AN ARC-HEATED,
HYPERSONIC, LOW-DENSITY WIND TUNNEL

By Ruth N. Weltmann

Lewis Research Center
Cleveland, Ohio

NATIONAL AERONAUTICS AND SPACE ADMINISTRATION
WASHINGTON

August 1962

NATIONAL AERONAUTICS AND SPACE ADMINISTRATION

TECHNICAL NOTE D-1169

DESIGN AND CALIBRATION OF AN ARC-HEATED, HYPERSONIC, LOW-DENSITY WIND TUNNEL

By Ruth N. Weltmann

SUMMARY

The design and calibration of an arc-heated gas jet that produces a continuous flow in a wind tunnel at a Mach number of 4 to 5 are described. Uniform flow conditions prevail over a central 1-inch-diameter core at static pressures of 0.05 to 0.1 millimeter of mercury with enthalpies up to 4300 Btu per pound for nitrogen and 1100 Btu per pound for argon. These conditions correspond to stagnation temperatures up to 9000° R, to altitudes of about 200,000 feet, and to velocities of about 11,000 feet per second.

Details are given for design features that produce stability of a confined arc over long periods of time with arc transfer efficiencies up to 50 percent. For nitrogen, the downstream gas jet is about 5 percent dissociated, and the vibrational energy is in equilibrium before the gas enters the nozzle throat.

Mass-averaged total downstream enthalpies, computed from profile measurements made with total-pressure probes and several stagnation-point heat-transfer probes of similar design about 1/4 inch downstream of the nozzle exit, agree within 10 percent with enthalpies computed from electric-power input, mass-flow rates, and coolant temperature rise. The enthalpies determined in the center core are about 20 percent higher.

INTRODUCTION

The theoretical and experimental study of high-energy, hypersonic, low-density gas flow and of the interaction with solid bodies is required for the solution of research problems in the areas of sustained flight at high altitudes, plasma and ion propulsion, reentry, and plasma-gas kinetics.

Methods for producing high-energy, hypersonic gas flows, such as shock tubes (ref. 1) and blowdown tunnels (ref. 2) that allow only a

fraction of a second for testing, sometimes provide limited information because of the transient nature of the flow, the practical difficulties involved in mapping the flow, and the dynamic lag of the instrumentation. Additional information is frequently desirable, which can only be obtained from continuous-flow devices like the wind tunnel. When a gas is sufficiently heated, a wind tunnel produces a steady gas stream of known energy content and composition, which can be sustained for long testing times. This type of continuous high-energy flow device can be used to determine gas properties, such as recombination and relaxation times, to study stagnation heat-transfer and ablation problems, and to develop new measuring techniques. An arc-powered plasma jet is one means of producing such a continuously operating, high-energy, hypersonic gas jet. Therefore, a direct-current arc jet was built and attached to the low-density facility described in reference 3. Other arc-heated, hypersonic jet tunnels are described in reference 4.

In this report, an arc-powered direct-current heat source for a hypersonic, low-density gas jet is described, and some of the problems encountered in its operation are indicated. Pressures and enthalpies in the jet are mapped after expansion through a Mach 4 nozzle, which has an exit diameter of 2.7 inches. Enthalpy comparisons made by stagnation-point heat-transfer measurements and heat-balance computations are also described. A discussion is presented of the change in the energy state of the gas as it flows from the arc heater to the low-density test section.

ARC HEATER

Arc Design

The arc heater, which is attached to the wall of the test chamber of the low-density facility, is shown in figure 1. The gas enters and expands through a Mach 4 nozzle, which in design is similar to the one described in reference 5. It is made of Inconel, has a throat diameter of 0.45 inch and an exit diameter of 2.7 inches and is designed to minimize the boundary-layer buildup. At room temperature with the available pumping facility, the jet has almost uniform flow, that is, flat pressure and enthalpy profiles across the 1-inch-diameter center core for mass flow rates ranging from 0.2 to 0.5 gram per second. These mass flow rates correspond to static pressures of 0.05 to 0.1 millimeter of mercury and to Pitot pressures (total pressures behind the normal shock) of 1 to 2 millimeters of mercury at the nozzle exit with upstream pressures of 6 to 15 millimeters of mercury in the plenum chamber. Since the arc heater is attached to the low-density facility upstream of the nozzle, the arc jet had to be discharged into the plenum chamber at pressures of 6 to 15 millimeters of mercury.

A direct-current arc was chosen for the heat source, because it is relatively simple to construct. A similar design was used by other investigators (refs. 4, 6, 7, and 8). The cathode is a water-cooled tube with a 1-percent thoriated-tungsten tip to minimize electrode wear and consequent gas contamination (ref. 4). The gas is introduced through an annulus that is concentric with the cathode and forms a vortex ahead of the tungsten tip, which assists in stabilizing the arc. The water-cooled copper anode contains a channel about 0.4 inch in diameter and 3 inches long to confine the arc. A water-cooled metal plenum chamber about 3 inches in diameter and about 6 inches long is provided between the anode exit and the nozzle throat for the purpose of gas mixing. The power input across the arc ranged from 2 to about 9 kilowatts with a maximum current of about 100 amperes.

Arc Stability

Since the nozzle throat and anode channel had about the same diameter, the anode upstream pressure, or the pressure in the arc chamber, was about the same as the plenum-chamber pressure. For the stated flow conditions, this pressure was in the range of 6 to 15 millimeters of mercury. In this pressure range, where the breakdown voltage is low, it was difficult to stabilize the arc for any length of time and to prevent it from jumping to adjacent metal surfaces. The pressure in the arc chamber was increased by inserting a copper orifice into the copper anode channel, which increased the breakdown voltage and stabilized the arc. An orifice of about 1/8-inch inside diameter proved best for the previously indicated gas-flow rates. With this orifice and with the arc off (i.e., at room temperature) the pressure in the arc chamber was increased to 150 to 400 millimeters of mercury. When the arc became stable, it formed a well-defined column, which could be observed through windows in the arc chamber.

Although the use of the orifice achieved arc stability in the arc chamber, the arc did not always seem to terminate at the anode but would frequently jump to the metal surface of the plenum chamber, again causing arc instability and loss of plasma energy in heat transfer to the walls of the chamber. In order to correct this situation, a thin-walled boron nitride cylinder of about 1-inch inside diameter was loosely inserted into the plenum chamber to act as a heat shield and to provide a mixing chamber (fig. 1). Boron nitride was chosen because it is resistant to high temperatures, it is an electric insulator, and it has relatively high thermal conductivity. The latter property proved to be important since it had been established that a ceramic cylinder of relatively low thermal conductivity must be externally heated to produce a plasma jet as stable as the one obtained by using the boron nitride cylinder insert. With a heated ceramic cylinder or a boron nitride cylinder inserted, the arc and plasma are stable and well confined, and the facility can be operated for hours.

Arc Starting

The arc is started with a third electrode, a thin copper wire, that evaporates after ignition. Additional lengths of wire can be fed into the chamber while it is under vacuum, so that multiple starts of the arc can be made without shutting down the facility.

Arc Operating Conditions

The input efficiency, or the power across the arc for a constant terminal power, increases with an increase in arc resistance; therefore, it is advantageous to have a long arc. The transfer efficiency, or the power that is transferred to the downstream gas jet for a constant power across the arc, increases with a decrease in heat loss due to heat transfer along the gas path; therefore, the transfer efficiency is highest for a well-confined arc. In this test facility, arc stabilization was achieved for long periods of time for arcs terminating upstream and downstream of the orifice or anode. The downstream condition is preferable, since then the stabilization seems to be of unlimited duration, and the efficiency of energy input and transfer to the downstream gas jet is highest because the arc is long and well confined within the anode and orifice. For an arc terminating downstream of the orifice, and therefore well confined, the transfer efficiency was about 35 to 55 percent of the energy input across the arc; whereas it often decreased to only 20 or 30 percent for a less-confined arc that terminated somewhere between the upstream surfaces of the orifice and anode. An arc of high transfer efficiency and sustained stabilization, which terminates downstream of the orifice or anode, is obtained only if the heat conduction between the water-cooled anode channel and the orifice is excellent, so that the orifice is uniformly cooled. Otherwise, the arc will terminate at any "hot spot" near the orifice upstream surface and become unstable by arcing to the nearest upstream surface of the anode. Even these arcs were stable over long enough periods of time to permit certain measurements.

Energies up to about 5000 Btu per pound were supplied to the nitrogen arc after deduction for heating losses in the electrodes. This energy range corresponds to arc temperatures of about 11,000° R and to a degree of dissociation of about 10 percent at near-atmospheric pressure. For the same energy input, arc drift velocities of about 3300 feet per second and ion and electron densities of about 5×10^{15} particles per cubic centimeter were calculated from the measured current density and voltage. This ion concentration is about correct for nitrogen at 11,000° R and at atmospheric pressure.

CALIBRATION TECHNIQUES AND INITIAL RESULTS

Calibration Problems

The conventional aerodynamic calibration techniques for measuring pressure and temperature to interpret the flow conditions in a test facility do not apply to low-density, high-enthalpy, high-velocity gas streams. For low-density conditions, the effects of low Reynolds numbers and slip flow, or free-molecule flow, have to be considered. At high temperatures, cooling of the calibration equipment becomes a necessity, which introduces problems of interpretation for heat-transfer measurements. As long as gas kinetics cannot be completely assessed, only enthalpy can be determined from heat-transfer-rate measurements. Temperatures can be obtained from enthalpy determinations only by assuming thermal equilibrium or by knowing the energy states of the gas. Other papers (refs. 9, 10, 11, and 12) have recently been published considering some of the problems of calibration in a high-energy, low-density, hypervelocity wind tunnel.

In this report, calibration techniques are described that use pressure and heat-transfer-rate measurements. Interpretation of flow properties in the upstream plenum chamber, in the nozzle, and in the downstream gas jet was made by applying the necessary corrections with an estimate of the uncertainty in corrections, wherever possible.

Upstream Plenum-Chamber Profiles

In order to measure static- and total-pressure profiles along the diameter of the plenum chamber at gas temperatures up to 9000°R , a special probe was built with a boron nitride tip to withstand the high surrounding gas temperatures by ablation cooling. Space limitations did not permit the use of an impact probe of conventional L-shaped design. The probe used is shown in figure 2. The boron nitride tip was machined and cemented into a stainless-steel tube of $1/4$ -inch outside diameter, which was inserted through a $1/4$ -inch vacuum coupling. The tube was motorized so that it could be moved up and down along the diameter of the plenum chamber. Care was taken to make the intake hole large enough (0.1 -in. diam.) to avoid erroneous results due to low Reynolds numbers (ref. 13). The probe served as an impact probe when the intake hole faced the gas stream and as a static probe when it was turned 90° . Two static wall taps were used, one in the heat shield and the other in the outside metal wall. Also, a conventional L-shaped impact probe was inserted to measure the total pressure between the outer wall and the heat shield. All upstream pressures were measured with manometers.

Typical profiles are shown in figure 3. The flow measured with all probes was in the continuum flow region; therefore, no pressure

corrections seemed necessary. The static-pressure profiles measured across the mixing chamber indicated constant static pressure. The same pressure was measured by the wall taps. At room temperature, the total-pressure profiles were identical (fig. 3(a)) when measured with or without the heat shield. The center Mach number is about 0.40 for both room-temperature profiles.

Without the heat shield, the arc could not be stabilized long enough to permit a pressure-profile measurement in the plenum chamber. The pressure profile with arc energy input and with the heat shield inserted is shown in figure 3(b). This pressure profile indicates that the jet velocity is relatively high at the centerline and that the total pressure decreases to the value of the static pressure (zero velocity) at the heat-shield walls. This profile also seems to indicate that most of the arc energy is contained within the gas center core and that a large boundary layer exists along the inside walls of the heat shield. The center-core Mach number is about 0.75, with $\gamma = 1.4$ assumed.

Downstream Jet Profiles

Pressure profiles across the downstream jet near the nozzle exit were measured with an impact probe and a static-pressure probe. Both probes had an outside diameter of 0.185 inch and an inside diameter of 0.120 inch. The impact probe had a 10° inside chamfer. Each probe was moved by an actuator, so that profiles could be taken across the nozzle, along the diameter, and at different distances from the nozzle exit. The probes were made of Inconel metal and were attached to a block of metal, which served as a heat sink and prevented overheating. Both the room-temperature and high-temperature pressure profiles are almost flat over about 1 inch in the center of the jet. A typical, high-temperature, Pitot-pressure profile is shown in figure 4. The profile was taken about $1/4$ inch downstream of the nozzle exit. Corrections to the pressure measurement made in the jet center core with the impact probe were not necessary, because the flow measured with this probe in the jet center core was always in continuum flow. No corrections for the impact pressure measurements in the boundary layer of the nozzle were made, since they were uncertain; thus, the profile boundary layer is considered to be only qualitatively correct. All measurements made with the static-pressure probe are in error, because the flow measured by this probe is always in the slip-flow region. According to reference 14, the error could be about 10 percent with an uncertainty of about 5 percent.

Profiles of heat-transfer rates are measured with a stagnation-point heat-transfer probe (ref. 15), which is shown in figure 5. The temperature difference between thermocouple positions 1 and 2 is a measure of the rate of heat transfer from the gas to the metal plug at the center of the probe, provided the plug is thermally insulated from the

other metal surfaces exposed to the gas. The rear of the plug is water cooled. Several probes were used that had the same cylindrical body radius but differed in nose radius. The distance between the two thermocouple positions differed in one probe. All dimensions are shown in the table in figure 5. For all probes, the plug was made of constantan, and the attached wires were made of Chromel. A third wire made of constantan (not shown) was embedded in the plug to permit absolute-temperature measurements at positions 1 and 2. The probes were mounted on two actuators to permit profile measurements across the jet and at different distances from the nozzle exit. It was possible to obtain actuator motion in both directions over about 4 inches. With two pressure probes and one stagnation-point heat-transfer probe mounted on the actuators, the probe centers were about $3/4$ inch apart. The pressure probes were combined (fig. 6) to determine whether or not one probe was interfering with the shock pattern of the other. This combined probe was placed $1\frac{1}{2}$ inches from the stagnation-point heat-transfer probe. Because the outside diameter of the static-pressure probe is large, about $3/8$ inch, it averages the static pressures over that distance; and, for this reason, it is used only for measuring the static pressures in the flat center of the jet profile. These static pressures checked fairly well with those measured at the nozzle wall near the exit by static-pressure taps and also checked the static pressures, measured previously with the separate static-pressure probe, for the same gas conditions. All downstream pressures were read on thermal-conductivity gages of the Pirani (Autovac) type.

A typical heat-transfer-rate profile with energy input is shown in figure 7 for nitrogen. The temperature difference ΔT measured between positions 1 and 2 in the constantan plug gives the rate $q = K \cdot \Delta T / X$ at which heat is transferred from the gas to the metal plug, where K is the thermal conductivity of constantan, and X is the distance between the thermocouple positions. Since ΔT and, therefore, the heat-transfer rate q are proportional to the square root of the Pitot pressure for otherwise constant conditions, the heat-transfer-rate profile is plotted in figure 7 as $q \sqrt{P_{O,c} / P_{O,l}}$. This expression presents a heat-transfer-rate profile similar to that obtained for a constant total pressure across the jet closely corresponding to the energy distribution in the jet. The heat-transfer-rate measurements were again taken about $1/4$ inch downstream of the nozzle exit; therefore, the Pitot pressures from figure 4 were used to change q into $q \sqrt{P_{O,c} / P_{O,l}}$. Study of the profile in figure 7 is made with the consideration that the measurements outside of the center core are uncertain because the corrections to the pressure measurements are uncertain and the heat-transfer-rate measurements are in error in the boundary layer, since the probe is located in a gas stream that has steep pressure and energy gradients across the probe stagnation surface. The object of presenting these profiles

(figs. 4 and 7) is to show that they are flat in the center over about 1 inch, which indicates the existence of a well-defined center core that might be considered isentropic.

Enthalpy Determinations

Enthalpies imparted to the gas jet were determined in two ways:
 (1) from the power input, the heat loss, and the gas mass-flow rate, and
 (2) from the heat-transfer rate and Pitot-pressure profiles measured 1/4 inch downstream of the nozzle exit.

In the first method, the power input into the gas is continuously measured by recording the voltage and current across the arc. When the arc is well stabilized, the current and voltage stay constant within 2 percent. The heat loss is obtained by monitoring the flow rates and temperatures of the cooling water passing through the electrodes, the plenum chamber, and the nozzle throat. Separate measurements were obtained for each of the four parts. The heat loss in the cathode is about 4 to 8 percent, in the anode 30 to 40 percent, in the plenum chamber 12 to 15 percent, and in the nozzle 6 to 10 percent. The total error in these measurements could be as high as 10 percent, but repeated measurements give a much smaller probable error. The gas-flow rate is measured continuously with a rotameter-type flowmeter. Total enthalpies H_0 are directly proportional to the power input into the arc after cooling losses divided by the mass-flow rate of the gas, plus the enthalpy of the gas at the gas inlet temperature.

In the second method, the heat-transfer rate q measured with the stagnation-point heat-transfer probe in the downstream gas jet was converted into enthalpy by using the Fay and Ridell equation (ref. 16), which has been derived for stagnation-point heat transfer by convection and diffusion to blunt bodies assuming laminar boundary-layer conditions. With a Lewis number of 1 assumed, the equation is

$$q = 0.763 \text{ Pr}^{-0.6} (\rho_w \mu_w)^{0.1} (\rho_o \mu_o)^{0.4} \sqrt{\frac{dv}{dx}} (H_o - H_w)$$

where w pertains to wall-temperature conditions at the stagnation probe and o pertains to stagnation-temperature conditions. The velocity gradient for Newtonian flow is

$$\frac{dv}{dx} = \frac{1}{R_N} \sqrt{\frac{2(p_o - p_s)}{\rho_o}}$$

and for hypersonic flow at $M > 3$, p_o is much greater than p_s and therefore

$$\frac{dv}{dx} = \frac{1}{R_N} \sqrt{\frac{2p_o}{\rho_o}}$$

Boison and Curtiss (ref. 17) have investigated experimentally the velocity gradient of stagnation around blunt bodies. They found that the equation for Newtonian flow is valid only for hemispherical bodies, and that the effective nose radius becomes smaller than the actual nose radius with increasing bluntness, so that the velocity gradient becomes

$$\frac{dv}{dx} = \frac{1}{R_{eff}} \sqrt{\frac{2p_o}{\rho_o}}$$

The effective radius was used in all enthalpy calculations and is listed in the table in figure 5.

Figure 8 is a plot of the simplified Fay and Ridell equation for nitrogen at pressure levels between 10^{-3} and 10^{-2} atmosphere, with stagnation-point heat-transfer-probe wall temperatures assumed between 600° and 800° R. The enthalpy difference $H_o - H_w$ is plotted against $q \sqrt{(R_{eff}/R)(p/p_o)}$ for $R = 1$ inch and $p = 1$ millimeter of mercury. Figure 8 can be used to obtain H_o from measurements of q with probes of any effective nose radius and for nitrogen at any pressure within the range indicated previously. The enthalpies were obtained from Mollier charts (ref. 18) and the transport properties from references 19 and 20. Figure 8 was used to convert the heat-transfer-rate profile of figure 7 into an enthalpy profile in figure 9.

The Fay and Ridell equation is based on the boundary-layer theory in complete continuum flow, and thus is correct only for high Reynolds numbers. References 21 and 22 show that the heat transfer to a hemispherical body, such as the nose of the stagnation-point heat-transfer probe, increases for Reynolds numbers at which the viscous effects become important in the layer between the shock and the body and that this occurs at Knudsen numbers that are considered to indicate continuum-flow conditions. The heat-transfer rate was found to be a maximum, about 20 percent higher than that based on the boundary-layer theory, at a Reynolds number for which the viscous layer extends to the shock region and affects the shock. For still lower Reynolds numbers, the heat-transfer rate was found to decrease to values based on the boundary-layer

theory and to approach the limiting value that is predicted from the free-molecule flow theory.

The stagnation Reynolds numbers, based on stagnation conditions and the radius of the stagnation-point heat-transfer probes, range from about 200 to 400 for the conditions discussed herein. This range of stagnation Reynolds number is in the range of maximum heat transfer where large viscous effects are present and increase the heat-transfer-rate measurement by 15 to 20 percent. Because the corrections are somewhat uncertain and the stagnation conditions can be obtained only by iteration, an average correction of about 18 percent was applied to the measured heat-transfer rates to obtain the corrected enthalpy profile shown in figure 9.

Again, the profile is presented to show the extent of uniform flow conditions in the jet center core. The enthalpy calculations through the boundary layer are questionable not only because of the uncertainties in pressure, Reynolds number, and heat-transfer-rate measurements, but also because figure 8, which was calculated using references 16 and 17, is based on heat transfer to the probe from gas of constant energy content over an area larger than the probe stagnation surface. The energy gradient across the stagnation surface of the probe, when it is in the boundary layer, will probably affect the velocity gradient dv/dx along the probe surface. For this reason, a calculation of the mass-averaged total enthalpy of the downstream gas jet, obtained by integration on the basis of these profiles (figs. 4, 7, and corrected 9), can be somewhat in error. Mass-averaged integrations indicate that the total enthalpy is about 20 percent less than the enthalpy in the center core of the jet.

Enthalpy Comparisons

In comparing enthalpies, the total heat input minus the total heat loss should be equal to the mass-averaged total heat content in the downstream jet. The enthalpies computed from heat-balance measurements check, within 10 percent, the mass-averaged total enthalpies in the downstream jet, which were obtained by mass-averaged integration using the Pitot-pressure profiles, such as those in figure 4, and the heat-transfer rate and corrected enthalpy profiles, such as those in figures 7 and 9, respectively. The measured range of heat balance and total downstream enthalpy extends from 900 to about 4300 Btu per pound for nitrogen. This agreement between the two enthalpy determinations (within 10 percent) over an extended range of enthalpies, although the measurements in the boundary layer are uncertain, seems to indicate that the stagnation-point heat-transfer probes are well suited to determine enthalpies in a low-density jet if the proper corrections are applied. The enthalpies computed from heat-transfer-rate and Pitot-pressure measurements in the uniform-flow center core should be even better than within 10 percent, because pressure and energy are constant across the core.

Two stagnation-point heat-transfer probes, the blunt-nose probe C and the flat-nose probe D, at first indicated about twice the heat-transfer rate corresponding to the heat-balance enthalpy. These high readings were probably caused by heat conduction from the edge, near the sonic point, to the constantan plug, thereby increasing the temperature of the thermocouple at position 1. This conclusion is based on the fact that readings, which were consistent with the other two probes, were obtained for both probes only after changing the fit of the plug into the body shield from a press fit to a slip fit to provide better heat insulation.

In low-density, hypersonic nozzle flow, the gas conditions are uniform over only a relatively small central part of the gas jet because of the presence of a large boundary layer. For nitrogen, in the present nozzle, this center core extends over about 1 inch as shown in figures 4, 7, and 9. Since this central core can be considered isentropic to permit calculations of gas kinetics and dynamics from only a few measurements, the enthalpy in the center core is of major interest in a low-density jet. Therefore, the enthalpies obtained from heat-transfer-rate measurements in the center core are compared with heat-balance enthalpies in figure 10 for nitrogen. The range of center-core enthalpy extends from 900 to 4300 Btu per pound and corresponds to a temperature range of 3000° to 9000° R with a degree of dissociation up to about 5 percent. Similar data have been obtained for argon with probe B, one of the blunt-nose probes, covering a range of enthalpy from 400 to 1100 Btu per pound corresponding to temperatures between 3000° to 9000° R. Figure 10 shows that the center-core enthalpies are about 20 percent higher than the mass-averaged total and heat-balance enthalpies, which could indicate that only part of the heat loss in the mixing chamber and nozzle is due to heat lost in the center core of the gas, while part of it is lost in cooling the two large boundary layers. Since the stagnation-point heat-transfer probes have metallic front surfaces, which are considered catalytic (ref. 23), the total heat-transfer rate could hardly be affected by whether or not the gas in the stagnation boundary layer is in equilibrium (ref. 16).

KINETIC GAS CONDITIONS

Gas Path

This discussion will be limited to nitrogen gas, which was used in most of the experiments. The state of the gas, in thermal equilibrium, depends on temperature and pressure and can be calculated by using the Mollier charts (ref. 18). Obtaining equilibrium requires time for the different energy modes to relax. These relaxation times τ are functions of temperature and density and can be found in the literature (refs. 24 and 25). Figure 11 is taken from these references and gives

the relaxation times for the vibrational modes and for dissociation and recombination of nitrogen as a function of temperature, referred to a density of 1 atmosphere. For the calculations, it is assumed, in accordance with reference 25, that the vibrational relaxation times are inversely proportional to the density, that the relaxation times for dissociation are inversely proportional to the $3/2$ power of the density, and that the relaxation times for recombination are inversely proportional to the square of the density. Ionization is not considered, since the ionization energies are negligible at the present gas conditions.

In this facility, the gas is heated by the arc in the arc chamber and moves through the anode, plenum chamber, and the nozzle to the test section to stagnate at the front surface of the measuring probe. During this process, the gas is cooled and undergoes an expansion in the nozzle. The state of the gas along its path is indicated in figure 12 for a typical enthalpy condition, with thermal equilibrium assumed. The gas in the arc loses energy through cooling of the electrodes. The gas in the center of the mixing chamber loses energy through cooling of both electrodes, the plenum chamber, and the nozzle. Since the downstream center-core energy is 20 percent higher than the total gas energy, the center-core energy in the mixing chamber is assumed to be also 20 percent higher than the total energy in the mixing chamber. If isentropic expansion through the nozzle is assumed (i.e., negligible heat loss in the jet center core as a result of heat transfer at the wall), entropy and total energy are preserved in the center core, but part of the energy is now transformed into kinetic energy. On stagnation, the gas regains the total energy. Figure 13 shows the temperature changes along the nozzle axis with isentropic expansion assumed through the nozzle for the condition indicated.

Figure 12 indicates that even at these relatively low temperatures the energy changes from one mode to another are quite substantial. Thermal equilibrium can occur only if the relaxation time τ is smaller than the flight time t , the time during which the state of the gas is required to change; that is, the relaxation time τ divided by the flight time t has to be smaller than unity for relaxation to occur. This ratio is plotted in figure 14 as a function of the gas path.

Inlet

The gas in the arc is about 10 percent dissociated, and some vibrational modes are excited. Figure 14 indicates that all the modes relax to a condition of thermal equilibrium in the arc as is expected; however, in the mixing chamber only the vibrational modes will relax because the flight time is too short for dissociation and recombination to occur. It is apparent from figure 14 that an increase in mixing-chamber length to obtain dissociation relaxation and recombination relaxation is not

feasible, because a completely impractical mixing-chamber length would be required for the given gas conditions. On the other hand, recombination of dissociated molecules occurs on all catalytic surfaces. Since the anode channel and orifice have large heated metallic surfaces, which are catalytic (ref. 23), sufficient recombination might occur at these surfaces with the result that the gas attains a state of thermal equilibrium in the mixing chamber.

Nozzle

The gas undergoes an expansion while passing from the throat to the exit of the nozzle. During expansion, the gas velocity increases while the gas temperature and pressure decrease, as indicated in figure 13. The expansion is rapid near the throat and levels off near the exit, causing nonlinear changes in the velocities and flight times as well as in the relaxation times as a function of nozzle length. For an exit pressure of 0.04 millimeter of mercury and at room temperature, the boundary-layer displacement thickness was calculated and experimentally checked in reference 5. Use of these data determined the pressure distribution along the nozzle axis for an exit pressure of 0.04 millimeter of mercury, with $\gamma = 1.4$ assumed. This pressure distribution was then scaled to the required exit pressure and was used together with figure 13(a) to plot figure 13(b), which shows the temperature as a function of nozzle length. This relation is not quite correct because of changes in γ , but it is believed to be a fair approximation of the temperature and pressure distribution along the nozzle axis for the indicated gas conditions. The curve of figure 13(b), with thermal equilibrium assumed throughout the nozzle, was used to calculate the flight and relaxation times along the nozzle length, which were used to plot figure 14. In this nozzle and at the given conditions the energies of dissociation and vibration do not relax at any point along the nozzle axis. In fact, it would be difficult to use a hypersonic nozzle of sufficient length to cause relaxation of the energy of dissociation during isentropic expansion at the given gas conditions.

Thus, the gas in the nozzle most likely is not in thermal equilibrium. It might be frozen at the equilibrium conditions of the mixing chamber or nozzle throat. The expansion through the nozzle with frozen conditions at the nozzle throat assumed is also shown in figure 13, for $\gamma = 1.4$ assumed, which again is not quite correct. The curves plotted in figure 13 indicate that the static temperature at the nozzle exit can be any temperature equal to or smaller than that obtained for thermal equilibrium, depending on the gas condition at which the energy state was frozen before expansion through the nozzle.

For stagnation enthalpies of about 3300 Btu per pound, for example, a Mach number of about 5 is calculated from the static and Pitot pressures

measured in the center and about 1/4 inch downstream of the nozzle exit, with $\gamma = 1.4$ assumed. This Mach number corresponds to a static temperature of about 2000° R at the nozzle exit with a gas velocity of about 10,000 feet per second. This nozzle-exit static temperature and gas velocity indicate that the gas energy was most likely frozen at the conditions of the mixing chamber or nozzle throat (fig. 13) for stagnation enthalpies of 3300 Btu per pound.

Stagnation

At stagnation, the state of the gas is not fully known. A stagnation-point heat-transfer probe with a catalytic surface does not distinguish between the different energies. It measures the heat-transfer rate from the sum of all energies, which corresponds to the enthalpy input for all gas conditions; whereas a probe with a noncatalytic surface measures the heat-transfer rate from the translational energy alone and thus measures lower enthalpies than correspond to the heat input, if the gas is in an excited state. Because the probes that were used had metallic catalytic surfaces, the measured heat-transfer rates correspond to the total energy of the gas jet independent of the kinetic condition of the gas at stagnation.

CONCLUDING REMARKS

In the wind tunnel facility described, stable operation of a confined arc was obtained by use of a uniformly cooled copper orifice in the anode channel; transfer efficiencies up to 50 percent were thereby obtained. The use of a boron nitride heat shield as a mixing-chamber liner helped to stabilize the arc and to create a large boundary layer. This boundary layer in the mixing chamber together with that in the nozzle seems to be responsible for confining a major part of the energy to the central core of the gas, with the result that the enthalpy in the center core is about 20 percent higher than the mass-averaged total downstream enthalpy.

For nitrogen, the length of the mixing chamber was sufficient to assure equilibrium of the vibrational energy modes at the nozzle-throat entrance. Computations and measurements indicate that some of the dissociated gas in the arc is probably recombined at the cooled, yet relatively hot, metallic surface of the anode and plenum chamber, since the gas seems to be in a state of thermal equilibrium before entering the nozzle, even though the flight time in the mixing chamber is too short to permit dissociation and recombination.

Calibration techniques so far developed give consistent results. The enthalpies calculated from electric-power input, mass-flow rates,

and coolant temperature rise check the mass-averaged total downstream enthalpies calculated from heat-transfer-rate and Pitot-pressure-profile measurements taken 1/4 inch downstream of the nozzle exit with impact-pressure probes and stagnation-point heat-transfer probes that have catalytic surfaces. Stagnation-point heat-transfer probes with different nose shapes were used, and the bluntness corrections as given in the literature were confirmed.

For the study of hypervelocity, low-density flow, only the uniform-flow center core of the gas jet is of interest. Therefore, it was advantageous to have most of the energy in this 1-inch diameter core. The velocities of the gas stream calculated from center-core enthalpies seem to be consistent with those obtained from pressure ratios. Static-temperature calculations, made from center-core enthalpies and pressure ratios, indicate that the gas is frozen at the mixing-chamber or nozzle-throat conditions.

Lewis Research Center
National Aeronautics and Space Administration
Cleveland, Ohio, June 18, 1962

APPENDIX - SYMBOLS

H	enthalpy
K	thermal conductivity in metal heat-transfer plug
ΔL	partial length of gas path of assumed constant energy conditions
M	Mach number
Pr	Prandtl number
p	pressure
q	heat-transfer rate to stagnation-point probe
R	radius of stagnation-point probe
T	absolute temperature
t	flight time, $\Delta L/v$
v	velocity
dv/dx	velocity gradient at stagnation around the probe nose
X	distance between thermocouple positions in stagnation-point heat-transfer probe
γ	specific-heat ratio
μ	viscosity
ρ	density
τ	relaxation time

Subscripts:

B	body of stagnation-point heat-transfer probe
c	center or core
eff	effective
l	local
N	nose of stagnation-point heat-transfer probe
o	total conditions, in supersonic flow behind normal shock
s	static conditions
w	conditions at wall of stagnation-point heat-transfer probe

REFERENCES

1. Hertzberg, A.: The Application of the Shock Tube to the Study of the Problems of Hypersonic Flight. *Jet Prop.*, vol. 26, no. 7, July 1956, pp. 549-554.
2. Perry, R. W., and McDermott, W. N.: Development of the Spark-Heated, Hypervelocity, Blowdown Tunnel - Hotshot. TR 58-6, Arnold Eng. Dev. Center, June 1958.
3. Weltmann, Ruth N., and Kuhns, Perry W.: Heat Transfer to Cylinders in Crossflow in Hypersonic Rarefied Gas Streams. NASA TN D-267, 1960.
4. John, Richard R., and Bade, William L.: Recent Advances in Electric Arc Plasma Generation Technology. *ARS Jour.*, vol. 31, no. 1, Jan. 1961, pp. 4-17.
5. Sreekanth, A. K.: Performance of a Mach 4 Axially Symmetric Nozzle Designed to Operate at 40 Microns Hg in the UTIA Low Density Wind Tunnel. Tech. Note 10, Inst. Aero., Univ. Toronto, Sept. 1956.
6. Finkelnberg, W., and Maecker, H.: Elektrische Bögen und thermisches Plasma. *Handbuch der Phys.*, vol. XXII, Springer-Verlag (Berlin) 1956, pp. 254-444.
7. Buhler, Rolf D.: Hyperthermal Research Tunnel Development and Transport Property Measurements, vol. I. *Plasmadyne Corp.*, PLR-66, Nov. 4, 1959.
8. Brogan, Thomas R.: The Electric Arc Wind Tunnel - A Tool for Atmospheric Re-Entry Research. *ARS Jour.*, vol. 29, no. 9, Sept. 1959, pp. 648-653.
9. Potter, J. Leith, Kinslow, Max, Arney, George D., Jr., and Bailey, A. B.: Description and Preliminary Calibration of a Low-Density, Hypervelocity Wind Tunnel. TN-61-83, Arnold Eng. Dev. Center, Aug. 1961.
10. Diaconis, N. S., and Warren, W. R.: Air Arc Simulation of Hypersonic Environments. Paper presented at Am. Rocket Soc. Int. Hypersonics Conf., M.I.T., Aug. 16-18, 1961.
11. Winkler, Ernest L., and Griffin, Roy N., Jr.: Effects of Surface Recombination on Heat Transfer to Bodies in a High Enthalpy Stream of Partially Dissociated Nitrogen. NASA TN D-1146, 1961.
12. Christensen, Daphne, and Buhler, Rolf D.: Arc Jet Measurements Related to Ablation Test Validity. Symposium on Reinforced Plastics for Rockets and Aircraft, Spec. Tech. Pub. 279, ASME, 1959.

13. Folsom, R. G.: Review of the Pitot Tube. Trans. ASME, vol. 78, no. 7, Oct. 1956, pp. 1447-1460.
14. Enkenhus, K. R.: The Design, Instrumentation and Operation of the UTIA Low Density Wind Tunnel. UTIA Rep. no. 44, Univ. Toronto, June 1957.
15. Krause, Lloyd N., Glawe, George E., and Johnson, Robert C.: Heat Transfer Devices for Determining the Temperature of Flowing Gases. Temperature - Its Measurement and Control in Sci. and Industry, vol. 3, pt. 2, Reinhold Pub., 1962, pp. 587-593.
16. Fay, J. A., and Ridell, F. R.: Theory of Stagnation Point Heat Transfer in Dissociated Air. Jour. Aero/Space Sci., vol. 25, no. 2, Feb. 1958, pp. 73-85; 121.
17. Boison, J. Christopher, and Curtiss, Howard A.: An Experimental Investigation of Blunt Body Stagnation Point Velocity Gradient. ARS Jour., vol. 29, no. 2, Feb. 1959, pp. 130-135.
18. Humphrey, R. L., Little, W. J., and Seeley, L. A.: Mollier Diagram for Nitrogen. TN 60-83, Arnold Eng. Dev. Center, May 1960.
19. Hilsenrath, Joseph, et al.: Tables of Thermal Properties of Gases. Cir. 564, NBS, Nov. 1, 1955.
20. Hirschfelder, Joseph O., Curtiss, Charles F., and Bird, R. Byron: Molecular Theory of Gases and Liquids. John Wiley & Sons, Inc., 1954.
21. Ferri, Antonio, and Zakkay, Victor: Measurements of Stagnation Point Heat Transfer at Low Reynolds Numbers. PIBAL 644, Polytechnic Inst. Brooklyn, Apr. 1961.
22. Cheng, H. K.: Hypersonic Shock-Layer Theory of the Stagnation Region at Low Reynolds Number. Proc. of 1961 Heat Transfer and Fluid Mech. Inst., Stanford Univ. Press, pp. 161-175.
23. Prok, G. M.: Nitrogen Atom Recombination on Surfaces. Physical Chemistry in Aerodynamics and Space Flight, A. L. Myerson and A. C. Harrison, eds., Pergamon Press, 1961.
24. Blackman, Vernon: Vibrational Relaxation of Oxygen and Nitrogen. Jour. Fluid Mech., pt. 1, vol. 1, no. 1, May 1956, pp. 61-85.
25. Logan, Joseph G., Jr.: Relaxation Phenomena in Hypersonic Aerodynamics. Preprint 728, Inst. Aero. Sci., Inc., 1957.

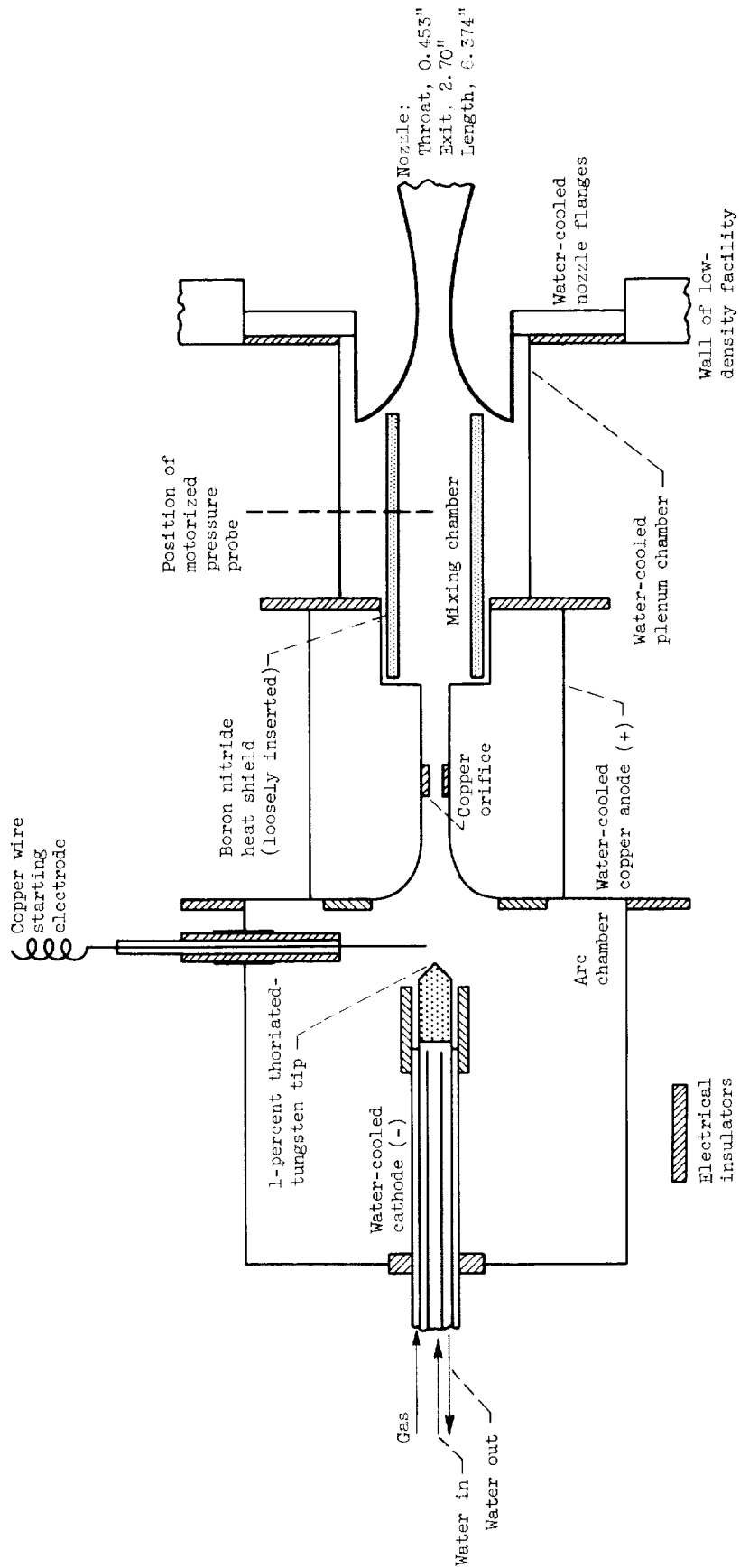


Figure 1. - Arc heater.

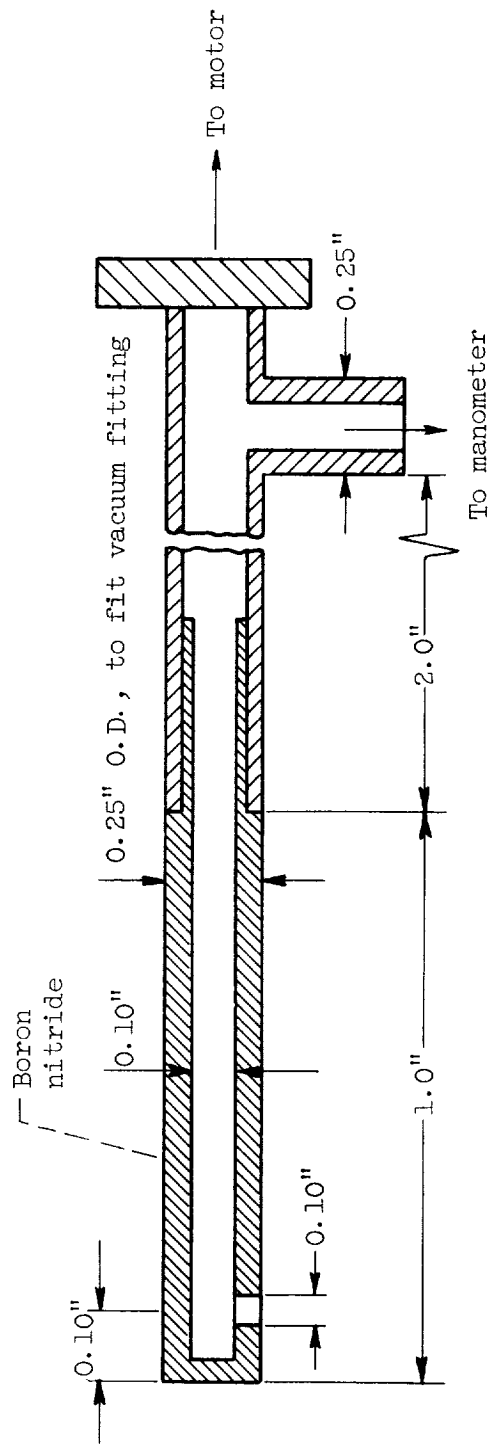
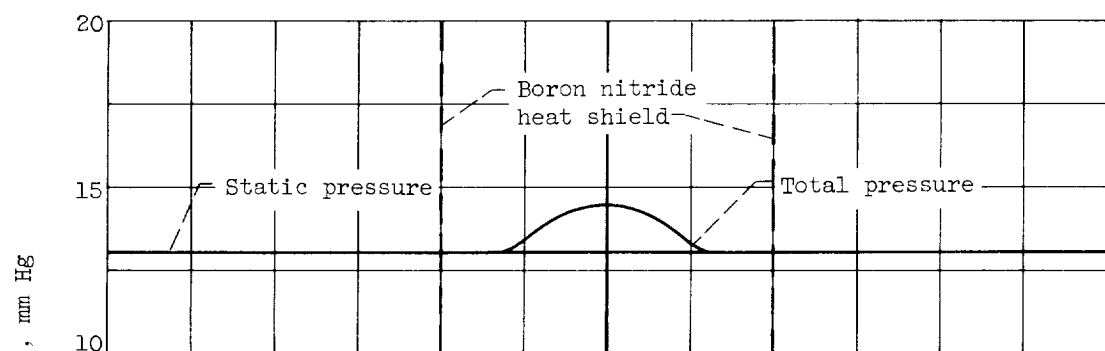
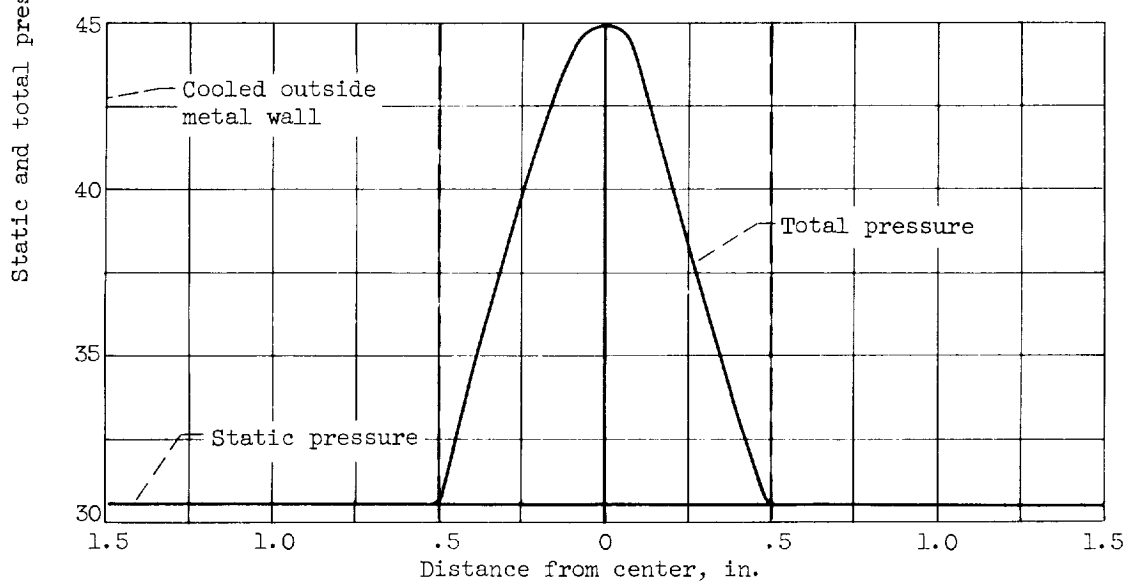


Figure 2. - Probe for measuring total- and static-pressure profiles in upstream mixing chamber.



(a) Room temperature. Center Mach number ≈ 0.40 .



(b) With arc energy input. Center Mach number ≈ 0.75 .

Figure 3. - Typical plenum-chamber pressure profiles.

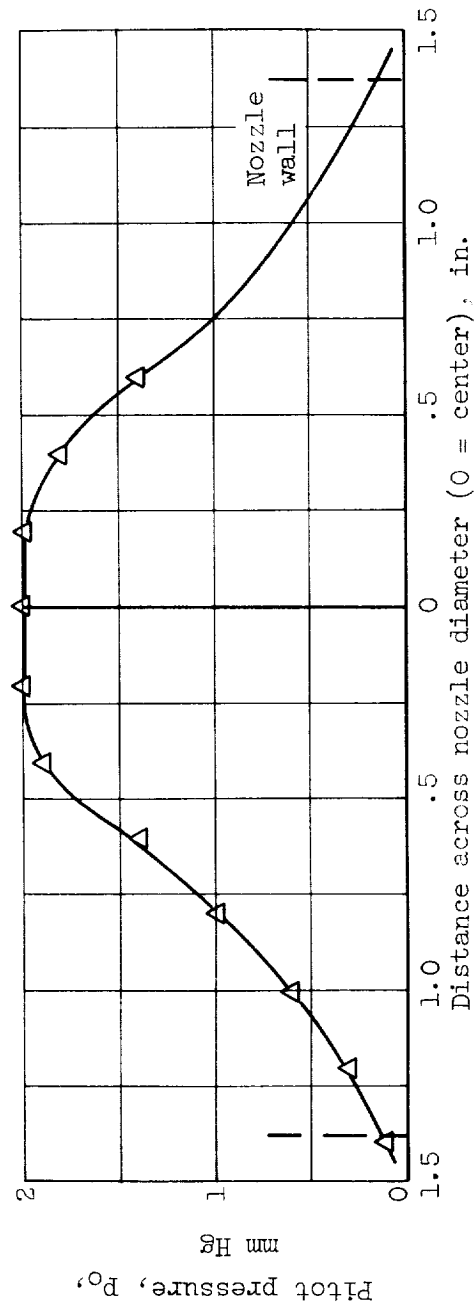
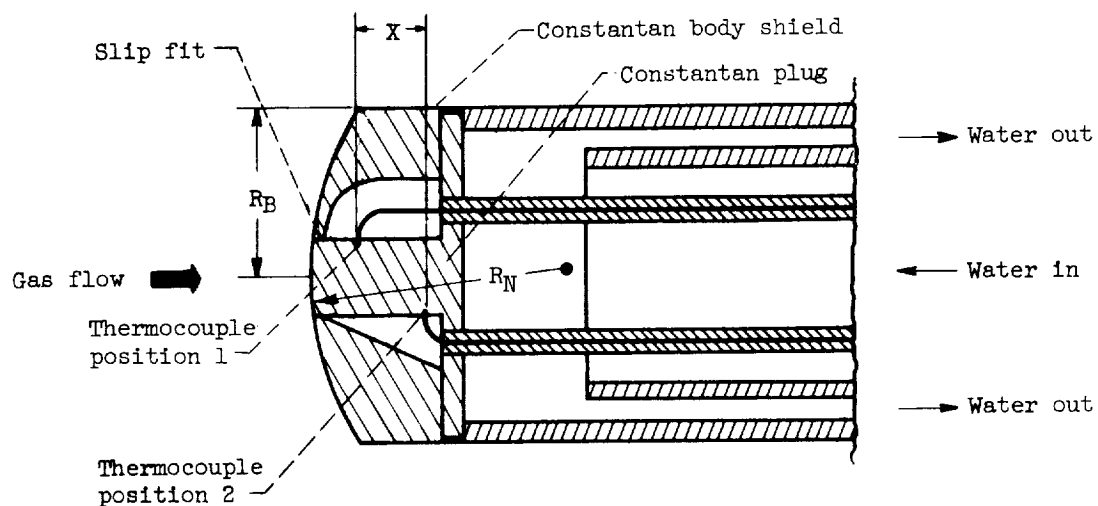


Figure 4. - Jet Pitot pressure profile with energy input taken 1/4 inch downstream of nozzle exit. Static pressure in jet center, 0.1 millimeter mercury.







Probe designation		Body radius, R_B , in.	Nose radius, R_N , in.	Effective radius, R_{eff}		Distance between thermocouple positions, X , in.
				Ref. 17	Present report	
A-hemisphere		0.25	0.25	$1.00 R_B$	0.25 in.	0.20
B-blunt		.25	.50	$2.24 R_B$.56 in.	.12
C-blunt		.25	.50	$2.24 R_B$.56 in.	.20
D-flat		.25	∞	$3.94 R_B$.98 in.	.20

Figure 5. - Stagnation-point heat-transfer probes (ref. 15).

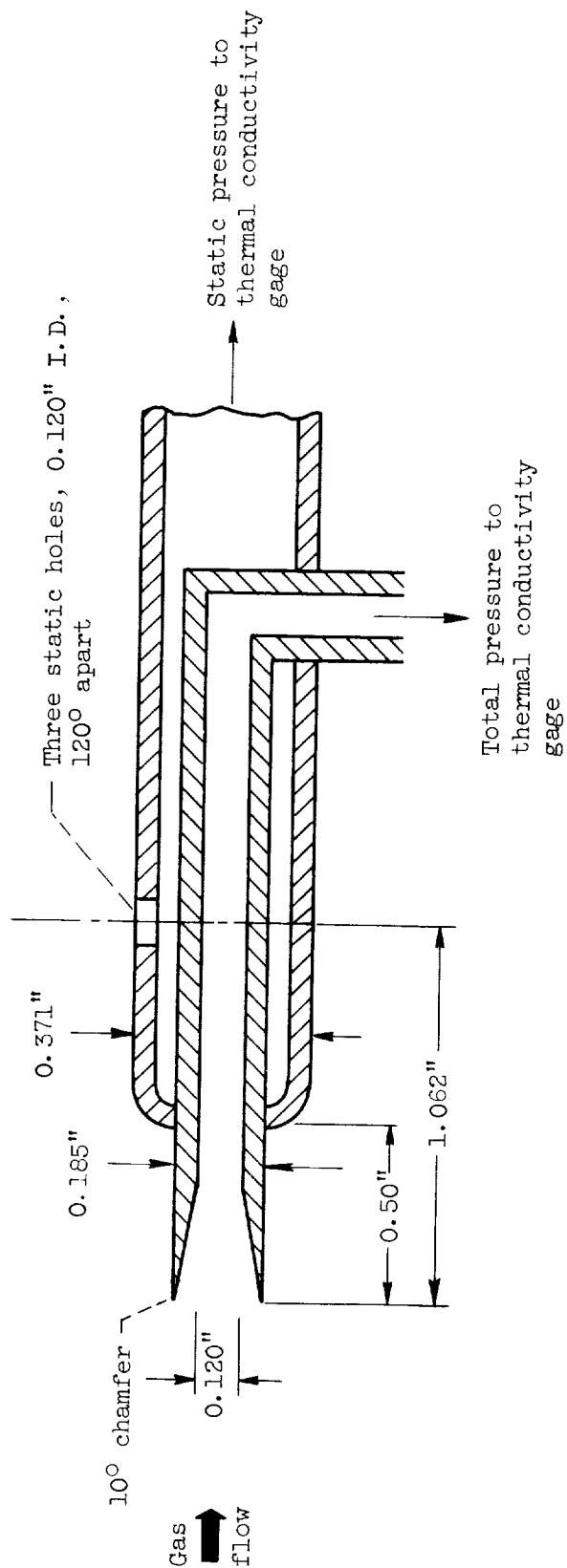


Figure 6. - Probe for measuring Pitot and static-pressure profiles in downstream jet.

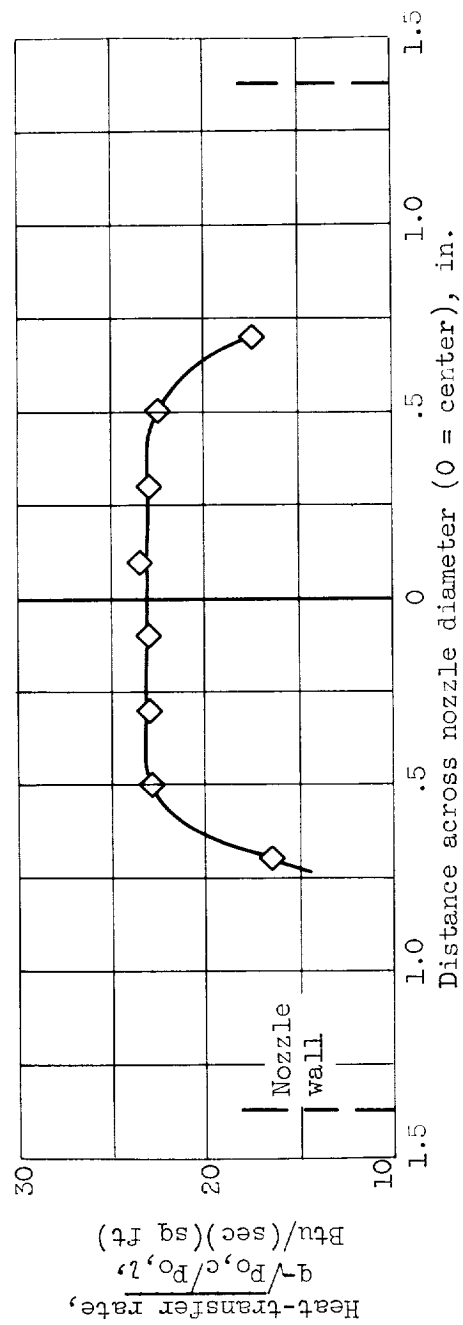


Figure 7. - Jet energy profile taken 1/4 inch downstream of nozzle exit. Pressures are taken from figure 4.

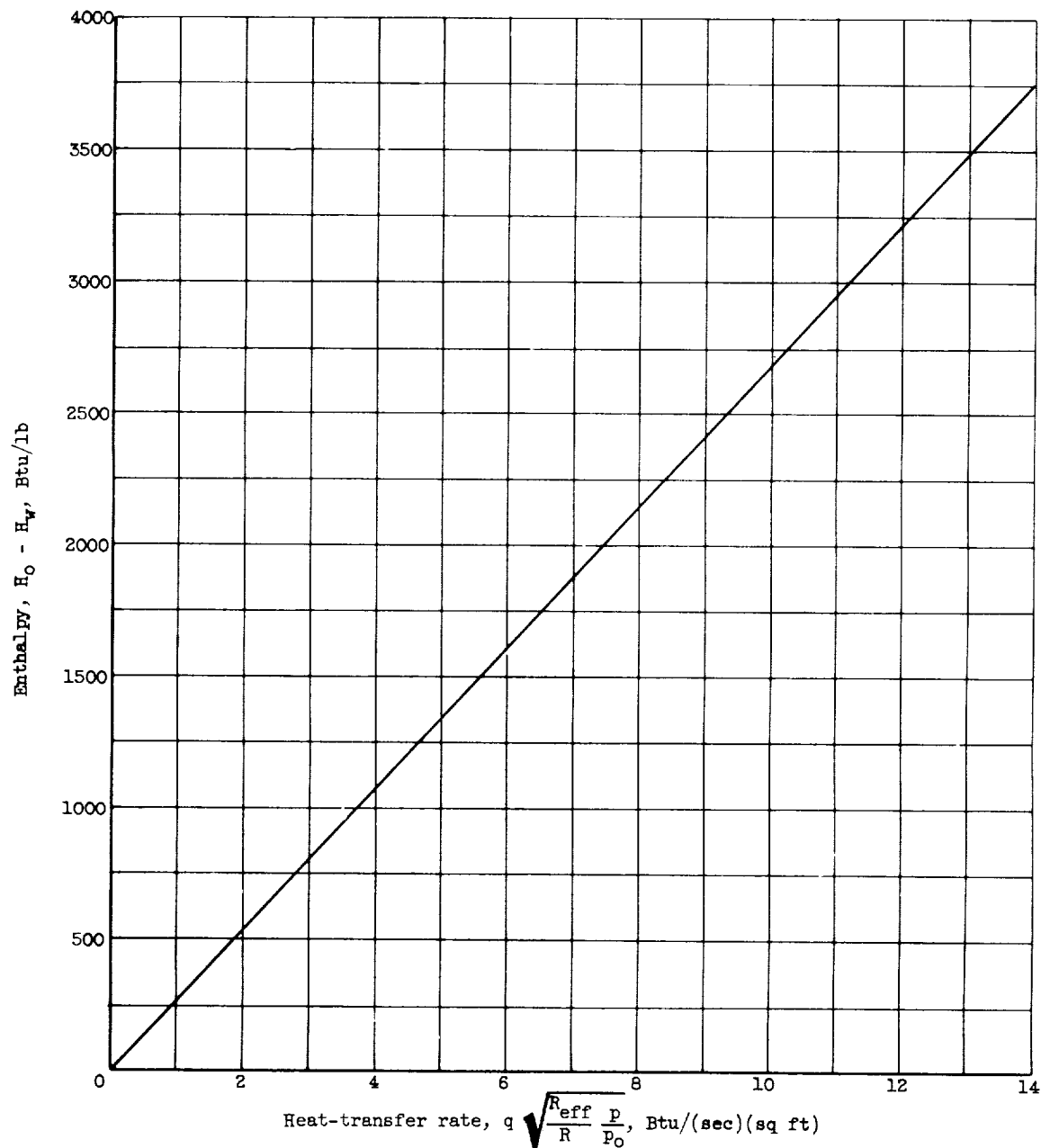


Figure 8. - Approximate relation between enthalpies and heat rates transferred to a stagnation-point probe. Calculated for nitrogen at: $10^{-3} < p_0 < 10^{-2}$ atmosphere; $600^\circ < T_w < 800^\circ$ R; $R = 1.0$ inch; $p = 1$ millimeter mercury.

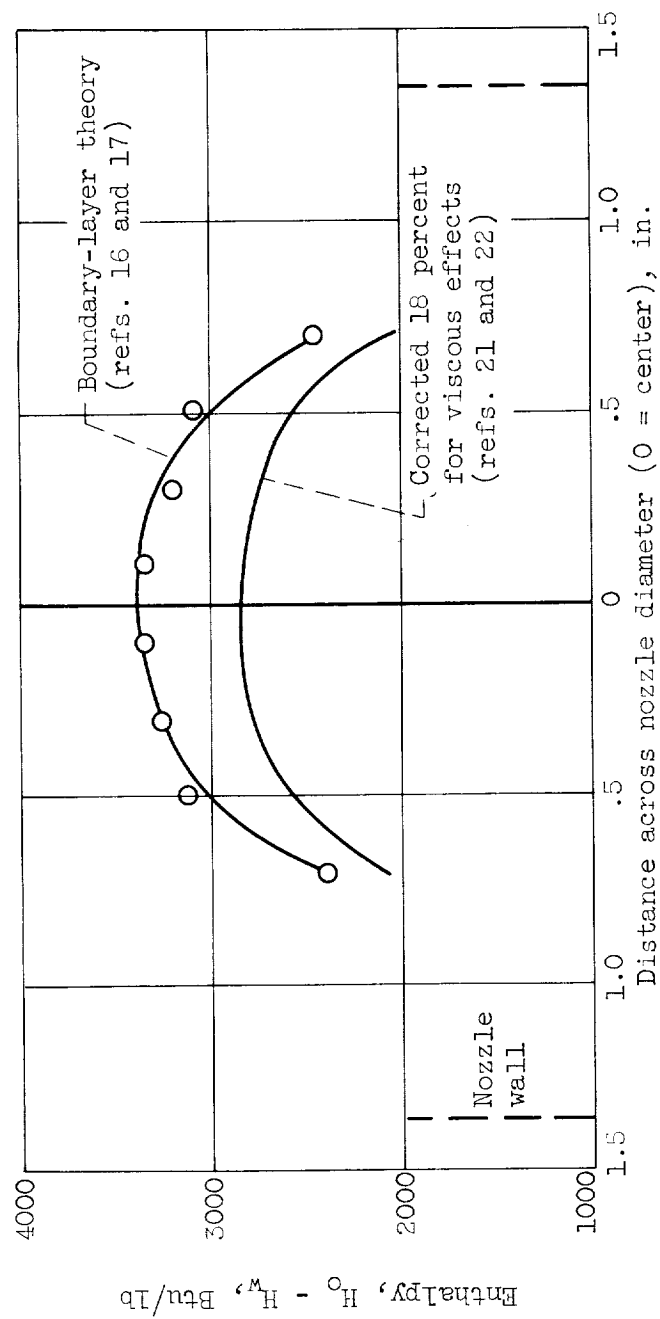


Figure 9. - Jet enthalpy profile taken 1/4 inch downstream of nozzle exit. Pressures and heat-transfer rates taken from figures 4 and 7, respectively.

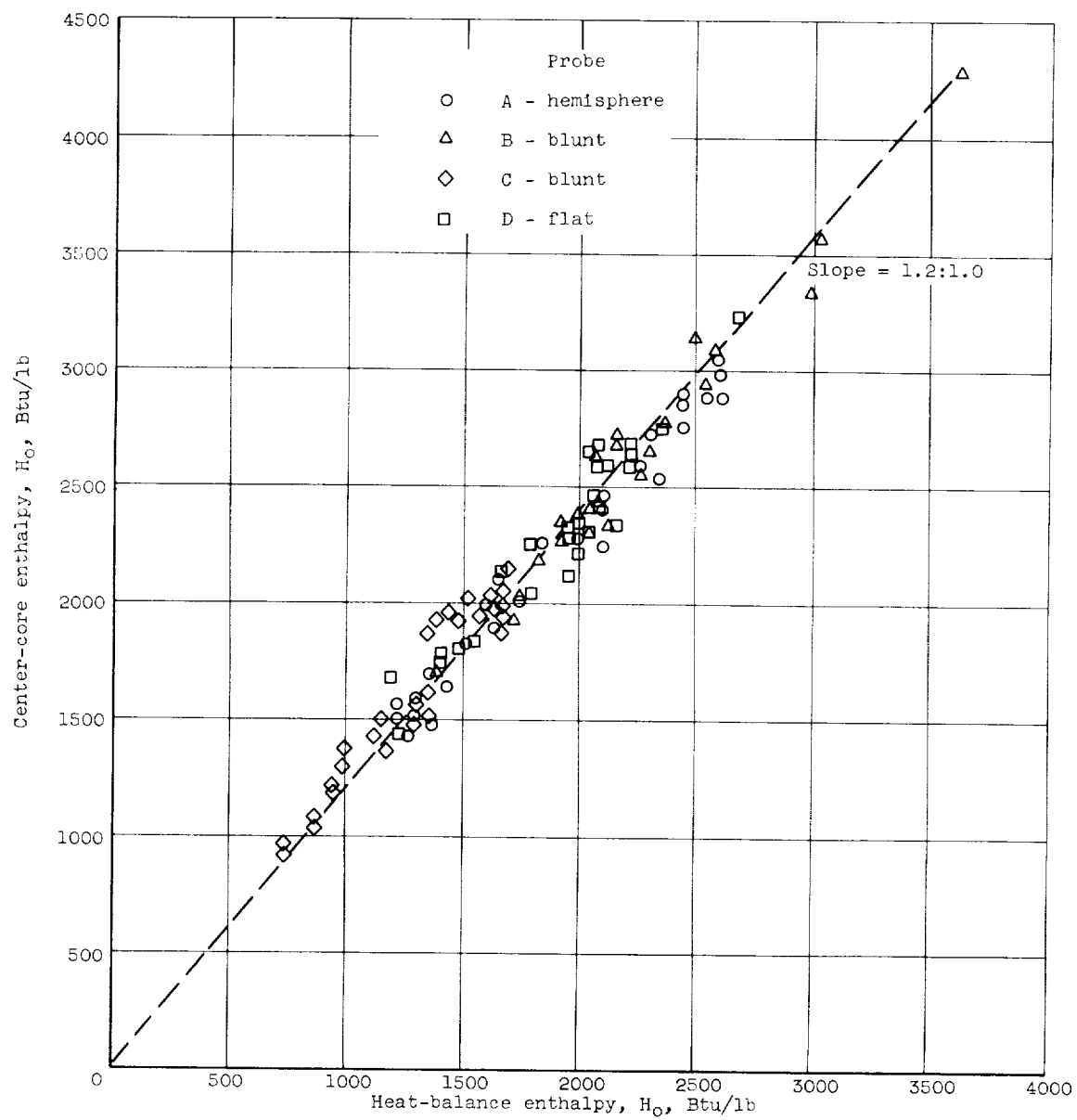


Figure 10. - Heat-balance enthalpy as function of enthalpy in center core for nitrogen.

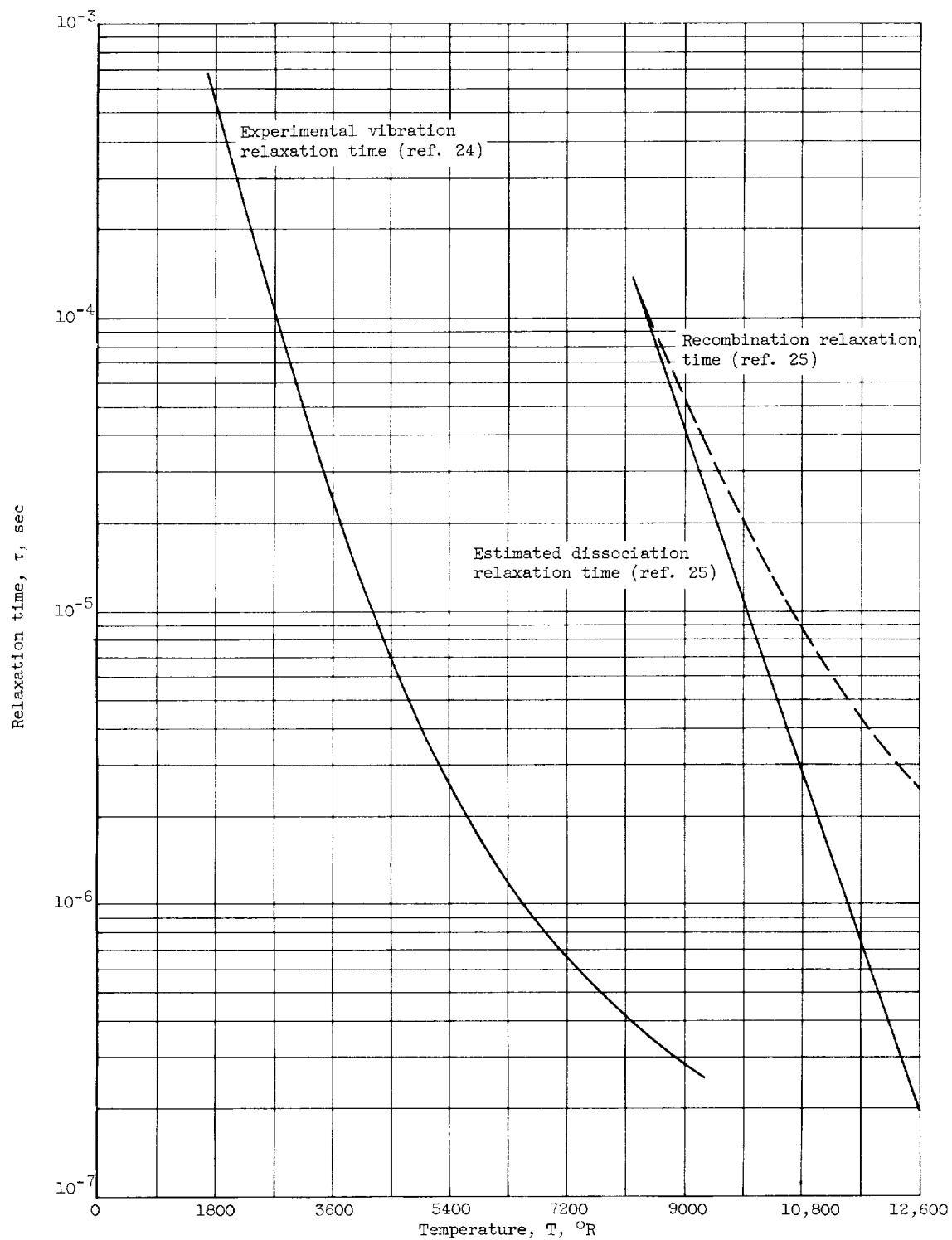


Figure 11. - Relaxation times for nitrogen referred to a density of 1 atmosphere.

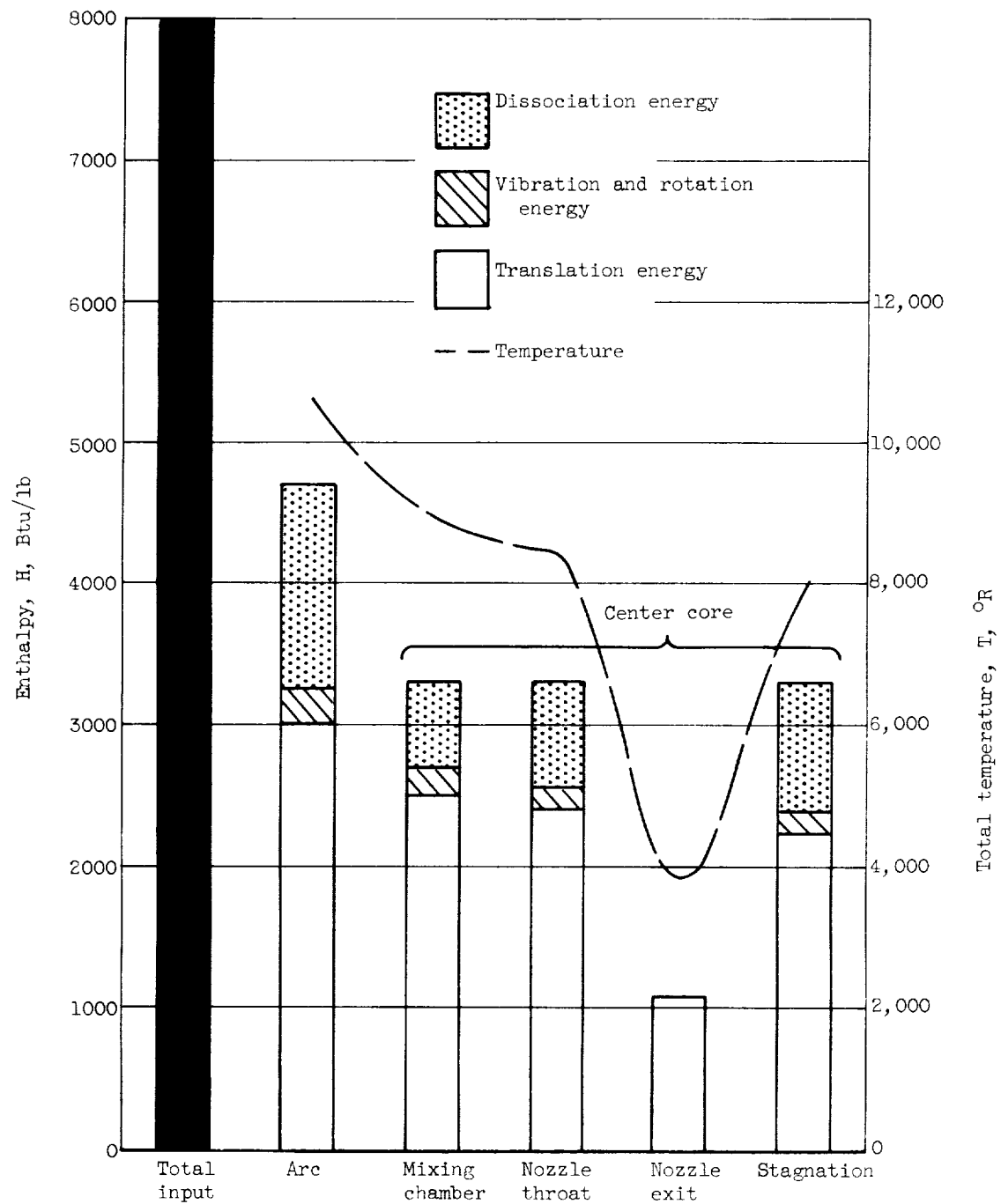
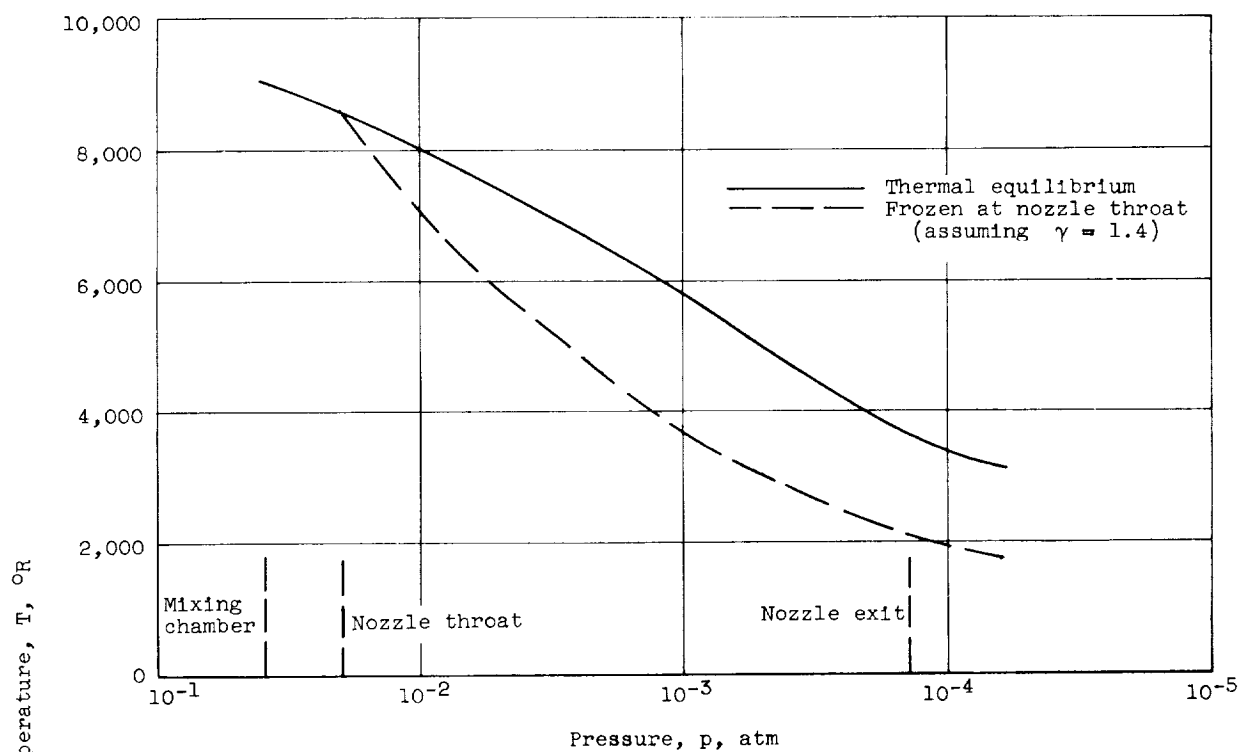
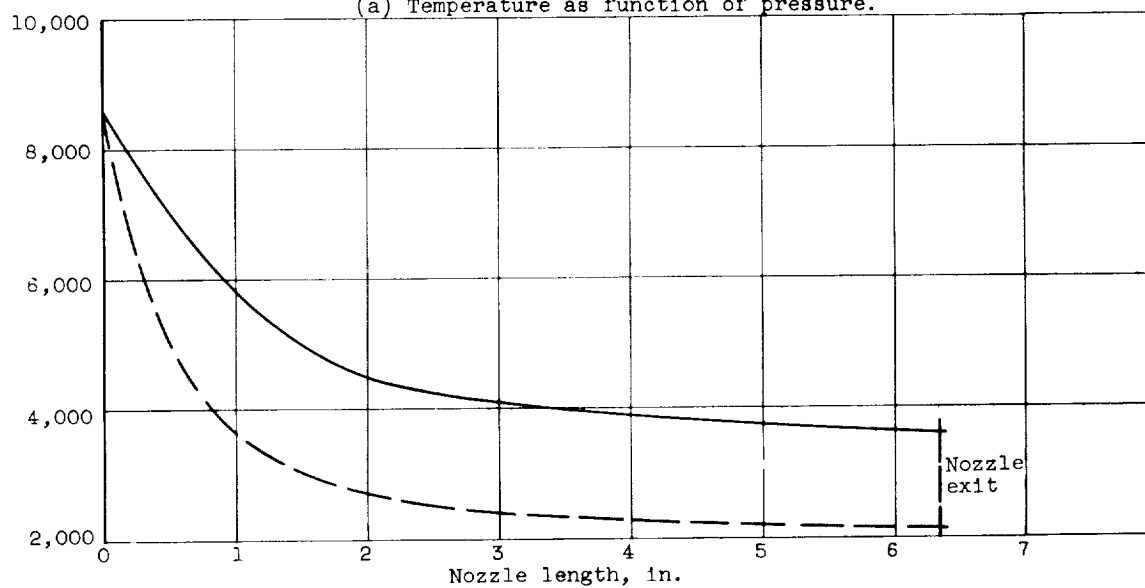


Figure 12. - Enthalpy and temperature along gas path with thermal equilibrium assumed.



(a) Temperature as function of pressure.



(b) Temperature as function of nozzle length (zero at nozzle throat).

Figure 13. - Expansion through hypersonic nozzle with isentropic conditions assumed.

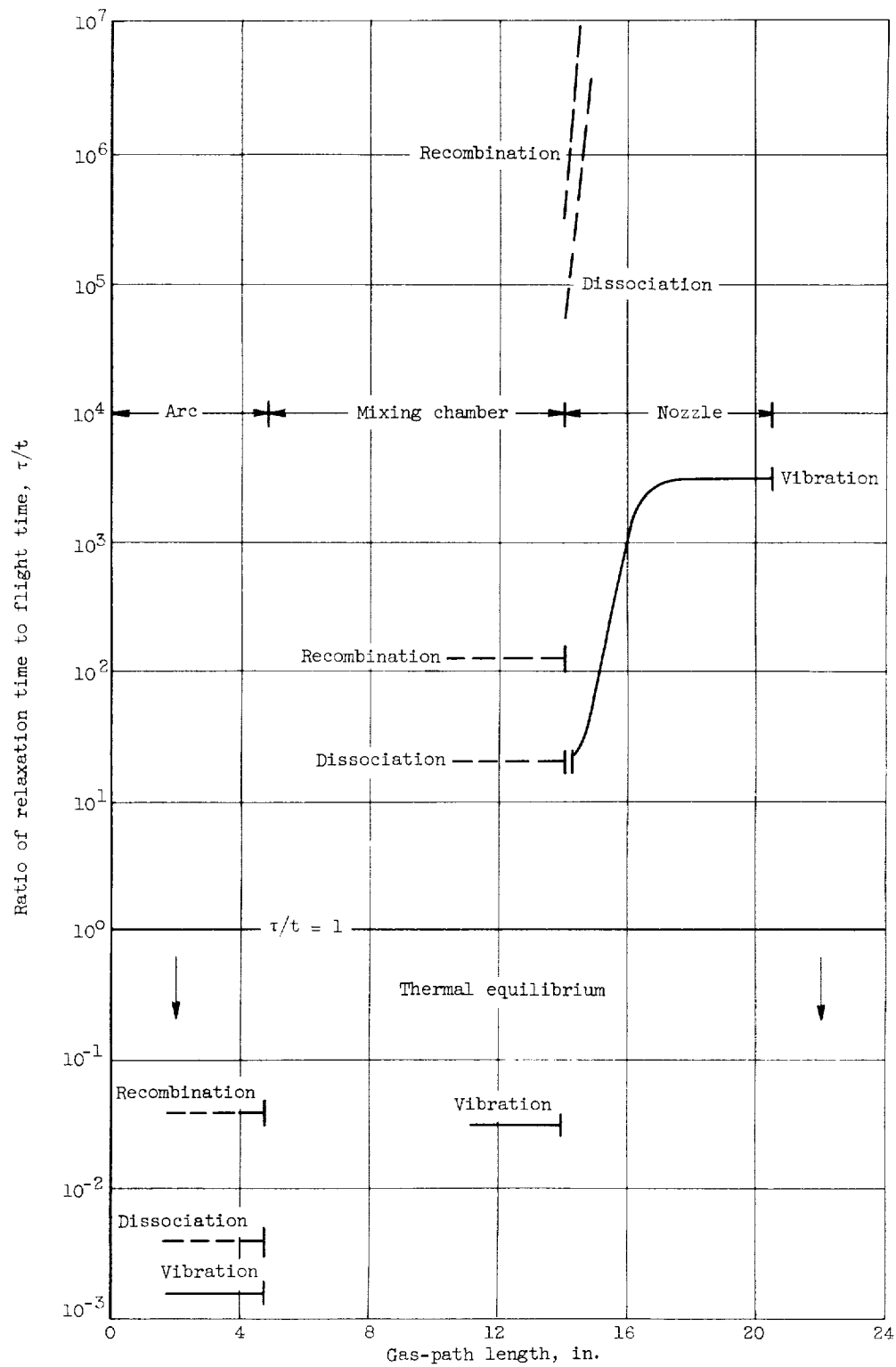


Figure 14. - Ratio of relaxation time to flight time as function of gas-path length.

<p>NASA TN D-1169 National Aeronautics and Space Administration. CALIBRATION TECHNIQUES IN AN ARC-HEATED, HYPERSONIC, LOW-DENSITY WIND TUNNEL. Ruth N. Weltmann. August 1962. 32p. OTS price, \$1.00. (NASA TECHNICAL NOTE D-1169)</p> <p>The design and calibration of a low-density gas jet are described that produce a continuous flow at Mach number 4 to 5 with uniform flow conditions over a 1-in.-diam. core and with enthalpies up to 4300 Btu/ lb for nitrogen, corresponding to stagnation tempera- tures up to 9000° R, altitudes of about 200,000 ft, and velocities of about 11,000 ft/sec. Details are given for design features that produce stability of a con- fined arc for continuous operation. Mass-averaged total downstream enthalpies, computed from profile measurements made with total-pressure and stagnation-point heat-transfer probes, agree within 10 percent with enthalpies computed from electric- power input, mass-flow rates, and coolant tempera- ture rise.</p>	<p>I. Weltmann, Ruth N. II. NASA TN D-1169</p> <p>(Initial NASA distribution: 2, Aerodynamics, missiles and space vehicles; 5, Atmospheric entry; 15, Chemistry, physical; 20, Fluid mechanics; 30, Physics, atomic and molecular; 37, Propulsion system elements; 41, Propulsion systems, electric; 45, Research and develop- ment facilities.)</p>	NASA
<p>NASA TN D-1169 National Aeronautics and Space Administration. CALIBRATION TECHNIQUES IN AN ARC-HEATED, HYPERSONIC, LOW-DENSITY WIND TUNNEL. Ruth N. Weltmann. August 1962. 32p. OTS price, \$1.00. (NASA TECHNICAL NOTE D-1169)</p> <p>The design and calibration of a low-density gas jet are described that produce a continuous flow at Mach number 4 to 5 with uniform flow conditions over a 1-in.-diam. core and with enthalpies up to 4300 Btu/ lb for nitrogen, corresponding to stagnation tempera- tures up to 9000° R, altitudes of about 200,000 ft, and velocities of about 11,000 ft/sec. Details are given for design features that produce stability of a con- fined arc for continuous operation. Mass-averaged total downstream enthalpies, computed from profile measurements made with total-pressure and stagnation-point heat-transfer probes, agree within 10 percent with enthalpies computed from electric- power input, mass-flow rates, and coolant tempera- ture rise.</p>	<p>I. Weltmann, Ruth N. II. NASA TN D-1169</p> <p>(Initial NASA distribution: 2, Aerodynamics, missiles and space vehicles; 5, Atmospheric entry; 15, Chemistry, physical; 20, Fluid mechanics; 30, Physics, atomic and molecular; 37, Propulsion system elements; 41, Propulsion systems, electric; 45, Research and develop- ment facilities.)</p>	NASA
<p>NASA TN D-1169 National Aeronautics and Space Administration. CALIBRATION TECHNIQUES IN AN ARC-HEATED, HYPERSONIC, LOW-DENSITY WIND TUNNEL. Ruth N. Weltmann. August 1962. 32p. OTS price, \$1.00. (NASA TECHNICAL NOTE D-1169)</p> <p>The design and calibration of a low-density gas jet are described that produce a continuous flow at Mach number 4 to 5 with uniform flow conditions over a 1-in.-diam. core and with enthalpies up to 4300 Btu/ lb for nitrogen, corresponding to stagnation tempera- tures up to 9000° R, altitudes of about 200,000 ft, and velocities of about 11,000 ft/sec. Details are given for design features that produce stability of a con- fined arc for continuous operation. Mass-averaged total downstream enthalpies, computed from profile measurements made with total-pressure and stagnation-point heat-transfer probes, agree within 10 percent with enthalpies computed from electric- power input, mass-flow rates, and coolant tempera- ture rise.</p>	<p>I. Weltmann, Ruth N. II. NASA TN D-1169</p> <p>(Initial NASA distribution: 2, Aerodynamics, missiles and space vehicles; 5, Atmospheric entry; 15, Chemistry, physical; 20, Fluid mechanics; 30, Physics, atomic and molecular; 37, Propulsion system elements; 41, Propulsion systems, electric; 45, Research and develop- ment facilities.)</p>	NASA
<p>NASA TN D-1169 National Aeronautics and Space Administration. CALIBRATION TECHNIQUES IN AN ARC-HEATED, HYPERSONIC, LOW-DENSITY WIND TUNNEL. Ruth N. Weltmann. August 1962. 32p. OTS price, \$1.00. (NASA TECHNICAL NOTE D-1169)</p> <p>The design and calibration of a low-density gas jet are described that produce a continuous flow at Mach number 4 to 5 with uniform flow conditions over a 1-in.-diam. core and with enthalpies up to 4300 Btu/ lb for nitrogen, corresponding to stagnation tempera- tures up to 9000° R, altitudes of about 200,000 ft, and velocities of about 11,000 ft/sec. Details are given for design features that produce stability of a con- fined arc for continuous operation. Mass-averaged total downstream enthalpies, computed from profile measurements made with total-pressure and stagnation-point heat-transfer probes, agree within 10 percent with enthalpies computed from electric- power input, mass-flow rates, and coolant tempera- ture rise.</p>	<p>I. Weltmann, Ruth N. II. NASA TN D-1169</p> <p>(Initial NASA distribution: 2, Aerodynamics, missiles and space vehicles; 5, Atmospheric entry; 15, Chemistry, physical; 20, Fluid mechanics; 30, Physics, atomic and molecular; 37, Propulsion system elements; 41, Propulsion systems, electric; 45, Research and develop- ment facilities.)</p>	NASA

